# Backscatter Modulation Design for Symbiotic Radio Networks



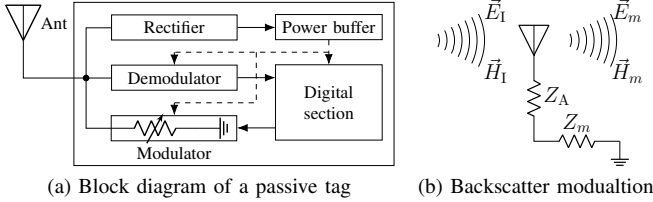(a) Block diagram of a passive tag    (b) Backscatter modualtion

Fig. 1. For a passive tag, the rectifier and demodulator rely on the incident electromagnetic wave for energy harvesting and source decoding, while the load-switcher adjusts the reradiated signal for backscatter modulation.

## I. BACKSCATTER MODEL

### A. Backscatter Principles

A bistatic backscatter system consists of an excitation source, multiple (semi-)passive tags, and a backscatter reader. When illuminated, the tags simultaneously harvest energy, backscatter message, and demodulate the source signal if necessary. Fig. 1(a) shows a typical passive with a scattering antenna, an energy harvester, an integrated receiver[1], a load-switching modulator, and on-chip components (e.g., micro-controller, memory, and sensors). A portion of the impinging signal is absorbed by the tag while the remaining is backscattered to the space. According to Green's decomposition [2], the backscattered signal can be decomposed into the *structural mode* component and the *antenna mode* component. The former is fixed and depends on the antenna geometry and material properties[2], while the latter is adjustable and depends on the mismatch of the antenna and load impedance. Fig. 1(b) illustrates a simplified circuit and backscatter model at tag state $m$. The corresponding reflection coefficient is defined as[3]

$$\Gamma_m = \frac{Z_m - Z_A^*}{Z_m + Z_A},\qquad(1)$$

where $Z_m$ is the load impedance at state $m$ and $Z_A$ is the antenna input impedance.

### B. Backscatter Modulation

Backscatter modulation is achieved by switching the tag load impedance between different states. For an $M$-ary Quadrature Amplitude Modulation (QAM) at state $m \in \mathcal{M} \triangleq \{1, \ldots, M\}$,

---

[1] For example, [1] prototyped a compact-size pulse position demodulator based on an envelope detector, which brings great potential to coordination, synchronization, and reflection pattern control.

[2] The structural mode component can be regarded as part of the environment multipath and modeled by channel estimation [3].

[3] We assume the linear backscatter model where the reflection coefficient is irrelevant to the incident electromagnetic field at the tag [4].
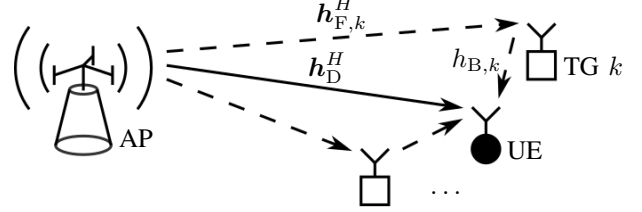
---



Fig. 2. A single-user multi-tag symbiotic radio system.

the reflection coefficient $\Gamma_m$ maps to the signal constellation point $\bar{c}_m$ as [5]

$$\Gamma_m = \alpha \frac{\bar{c}_m}{\max_{m'} |\bar{c}_{m'}|},\qquad(2)$$

where $\alpha \in [0, 1]$ is the reflection efficiency at a given direction. For simplicity, we consider an $M$-ary Phase Shift Keying (PSK) with constellation set $\mathcal{C} \triangleq \{\bar{c}_1, \ldots, \bar{c}_M\}$, where the $m$-th constellation point is

$$\bar{c}_m = \exp\left(j\frac{2\pi m}{M}\right).\qquad(3)$$

**Remark 1.** *For passive tags, the reflection efficiency $\alpha$ controls the tradeoff between the harvestable power and backscatter strength: $\alpha = 0$ corresponds to maximum power transfer to the tag, while $\alpha = 1$ with $M$-PSK corresponds to ideal Intelligent Reflecting Surface (IRS) with $M$ discrete states.*

## II. THE MULTI-TAG CASE

### A. System Model

As shown in Fig. 2, we propose a single-user (UE) multi-tag (TG) symbiotic radio network where the RF signal generated by the $Q$-antenna Access Point (AP) is shared by two coexisting systems. In the primary downlink system, the AP transmits information to the single-antenna user. In the secondary backscatter system, the AP acts as the carrier emitter, the $K$ nearby single-antenna tags modulate their information over the reradiated RF signals, and the user serves as the multi-tag backscatter reader. Denote the AP-UE direct channel as $\boldsymbol{h}_D^H \in \mathbb{C}^{1 \times Q}$, the AP-TG $k \in \mathcal{K} \triangleq \{1, \ldots, K\}$ forward channel as $\boldsymbol{h}_{F,k}^H \in \mathbb{C}^{1 \times Q}$, the TG $k$-UE backward channel as $h_{B,k}$, and the cascaded forward-backward channel of tag $k$ as $\boldsymbol{h}_{C,k}^H \triangleq h_{B,k}\boldsymbol{h}_{F,k}^H \in \mathbb{C}^{1 \times Q}$. For simplicity, we consider a quasi-static block fading model where the channel coefficients remain constant within each coherence interval and vary independently over different coherence intervals, and assume the coherence interval $T$ is much longer than the backscatter symbol period $T_c$ and primary symbol period $T_s$. We also assume the direct channel and all cascaded channels can be successfully estimated

and fed back to the AP.[4] Since the tags need to physically switch the loads for backscatter modulation, they communicate at a much longer symbol period (and lower rates) than the primary system. As such, we assume the transitions of all tags are perfectly synchronized, and the backscatter symbol period satisfies $T_c = NT_s$ where $N \gg 1$ is a positive integer.

Without loss of generality, we focus on the transmissions and detections during one particular backscatter symbol period. To provide a preliminary insight, we assume the primary symbol $s[n]$ at block $n \in \mathcal{N} \triangleq \{1, \ldots, N\}$ is in standard CSCG distribution, and the backscatter symbol $c_k$ of tag $k$ employs $M$-PSK modulation by (3), i.e., $c_k \in \mathcal{C}$, $\forall k \in \mathcal{K}$. Thus, the signal received by the user at block $n$ can be expressed as[5]

$$y[n] = \left( \boldsymbol{h}_D^H + \sum_{k \in \mathcal{K}} \sqrt{\alpha_k} \boldsymbol{h}_{C,k}^H c_k \right) \boldsymbol{w} s[n] + w[n], \quad (4)$$

where $\boldsymbol{w} \in \mathbb{C}^{Q \times 1}$ is the active precoder satisfying $\|\boldsymbol{w}\|^2 \leq P$, $P$ is the average transmit power constraint at the AP, and $w[n] \sim \mathcal{CN}(0, \sigma_w^2)$ is the equivalent Additive White Gaussian Noise (AWGN) at block $n$. Besides, we collect the backscatter symbols of $K$ tags into $c_{\mathcal{K}} \triangleq \{c_k : k \in \mathcal{K}\}$, stack the received signal over $N$ blocks as $\boldsymbol{y} \triangleq [y[1], \ldots, y[N]]^T \in \mathbb{C}^{N \times 1}$, and define the equivalent channel for primary transmission as

$$\boldsymbol{h}_E^H(c_{\mathcal{K}}) \triangleq \boldsymbol{h}_D^H + \sum_{k \in \mathcal{K}} \sqrt{\alpha_k} \boldsymbol{h}_{C,k}^H c_k. \quad (5)$$

**Remark 2.** *The proposed symbiotic radio system includes a multiplicative Multiple Access Channel (MAC) where the AP and the tags simultaneously transmit to the user. It inspired [TODO] to perform Successive Interference Cancellation (SIC) that first non-coherently detects the primary message under backscatter uncertainty, then cancels its contribution and decodes the tag messages. This scheme requires non-coherent coding at the AP and $K$ re-encoding, precoding, and subtraction operations at the user. However, different from the conventional MAC with Superposition Coding (SC), the symbiotic radio system involves Multiplication Coding (MC) that combines the primary and secondary messages by multiplication. Hence, novel multi-stream detection techniques should be tailored to symbiotic radio systems to accommodate the massive connectivity of tags and the multiplicative combination of links.*

### B. Backscatter Detection

To reveal the impact of backscatter modulation on the primary transmission, we extend the non-coherent Ambient Backscatter Communications (AmBC) detection [11] to the multi-tag case, and propose a low-complexity energy detection to decode the backscatter symbols under primary source uncertainty. It requires no dedicated receivers or non-coherent

codes at the AP, and can be readily implemented over legacy downlink systems.

**Remark 3.** *One key property of symbiotic radio is the primary message propagates to the user from a known channel and multiple multiplicative channels with uncertainty introduced by backscatter modulation. As such, each reflection coefficient simultaneously encodes the tag message and influences the equivalent channel of the primary link. If the backscatter symbols can be successfully decoded first, they can be modeled within the equivalent channel* (5) *as in channel training, instead of being removed by SIC.*

To explicitly specify each backscatter symbol combination, we label it by the corresponding modulation index set. For tag $k$ at state $m_k \in \mathcal{M}$, $\forall k \in \mathcal{K}$, we define the modulation index set as $m_{\mathcal{K}} \triangleq \{m_k : k \in \mathcal{K}\}$ and the tag input combination as $\bar{c}_{m_{\mathcal{K}}} \triangleq \{\bar{c}_{m_k} : k \in \mathcal{K}\}$. Since any $\bar{c}_{m_{\mathcal{K}}}$ remains constant per $N$ primary symbols, the received signal at block $n$ is only subject to the variation of the primary source $s[n]$ and AWGN $w[n]$, and thus follows CSCG distribution $y_{m_{\mathcal{K}}}[n] \sim \mathcal{CN}\left(0, \sigma_{m_{\mathcal{K}}}^2\right)$ with variance

$$\sigma_{m_{\mathcal{K}}}^2 = \underbrace{\left| \left( \boldsymbol{h}_D^H + \sum_{k \in \mathcal{K}} \sqrt{\alpha_k} \boldsymbol{h}_{C,k}^H \bar{c}_{m_k} \right) \boldsymbol{w} \right|^2}_{\boldsymbol{h}_E^H(\bar{c}_{m_{\mathcal{K}}})} + \sigma_w^2, \quad (6)$$

which denotes the expectation of the received power per primary block under tag modulation index set $m_{\mathcal{K}}$, and can be numerically evaluated based on the precoder, tag, channel, and noise knowledge. For the ease of exposition, we sort all possible $\sigma_{m_{\mathcal{K}}}^2$ in ascending order by a one-to-one mapping $m_{\mathcal{K}} \mapsto i$, denote the hypothesis that the tag input combination at status $i$ as $\mathcal{H}_i$, and define $\sigma_i^2 \leq \sigma_j^2$ for $i < j$, $i, j \in \mathcal{M}^{\mathcal{K}} \triangleq \{1, \ldots, M^K\}$.[6] For the optimal Maximum-Likelihood (ML) detector, the likelihood ratio between hypotheses $\mathcal{H}_i$ and $\mathcal{H}_j$ is [11]

$$\Lambda_{i,j}(\boldsymbol{y}) = \frac{f(\boldsymbol{y} \mid \mathcal{H}_i)}{f(\boldsymbol{y} \mid \mathcal{H}_j)} = \left( \frac{\sigma_j^2}{\sigma_i^2} \right)^N \exp \left( \frac{\sigma_i^2 - \sigma_j^2}{\sigma_i^2 \sigma_j^2} z \right), \quad (7)$$

where $f(\boldsymbol{y} \mid \mathcal{H}_i)$ and $f(\boldsymbol{y} \mid \mathcal{H}_j)$ are respectively the conditional probability density function of receiving $\boldsymbol{y}$ under hypothesis $\mathcal{H}_i$ and $\mathcal{H}_j$, and $z \triangleq \|\boldsymbol{y}\|^2$ is the received signal energy over $N$ primary blocks. Obviously, the likelihood ratio only depends on $z$ and the energy detection is thus optimal. The corresponding decision rule is

$$\Lambda_{i,j}(z) \underset{\mathcal{H}_j}{\overset{\mathcal{H}_i}{\lessgtr}} 1 \iff z \underset{\mathcal{H}_j}{\overset{\mathcal{H}_i}{\lessgtr}} T_{i,j}, \quad (8)$$

where the detection threshold between $\mathcal{H}_i$ and $\mathcal{H}_j$ is

$$T_{i,j} \triangleq N \frac{\sigma_i^2 \sigma_j^2}{\sigma_i^2 - \sigma_j^2} \log \frac{\sigma_i^2}{\sigma_j^2}. \quad (9)$$

Accordingly, the decision region of hypothesis $\mathcal{H}_i$ is

$$\mathcal{R}_i \triangleq [T_{i-1,i}, T_{i,i+1}), \quad (10)$$

---

[4]Due to the lack of RF chains at the passive tag, accurate and efficient Channel State Information at the Transmitter (CSIT) acquisition can be challenging. One possible approach is that the AP sends pre-defined pilots, the tags respond in well-designed manners, and the user performs least-square estimation with feedbacks [6]–[8].

[5]We omit the signal reflected by two or more times [9] and assume the time difference of arrival from different paths are negligible [10].

[6]When more than one modulation index sets yield the same energy level, the mapping is not unique and the detection fails to separate them. This blind spot issue can be mitigated by multi-antenna techniques.

and we manually define $T_{0,1} \triangleq 0$ and $T_{M^K,M^K+1} \triangleq \infty$. Let $f(z \mid \mathcal{H}_i)$ be the conditional probability density function of receiving $z$ under hypothesis $\mathcal{H}_i$. Correspondingly, $z$ is the sum of $N$ i.i.d. exponential variables each with mean $\sigma_i^2$, and thus follows Erlang distribution with shape $N$ and scale $\sigma_i^2$

$$f(z \mid \mathcal{H}_i) = \frac{z^{N-1}e^{-z/\sigma_i^2}}{\sigma_i^{2N}(N-1)!}. \tag{11}$$

On top of (25) and (11), we can formulate an equivalent point-to-point discrete memoryless channel from tag input combination alphabet $\mathcal{M}^K$ to received energy level alphabet $\mathcal{M}^K$ as a transition matrix, where the probability of observing energy level $j$ under tag input combination $i$ is[7]

$$P(\bar{z}_j \mid \bar{c}_i) = P(z \in \mathcal{R}_j \mid \mathcal{H}_i) = \int_{\mathcal{R}_j} f(z \mid \mathcal{H}_i)\mathrm{d}z. \tag{12}$$

Based on the equivalent point-to-point channel (12), we can compute the marginal probability on all tags and obtain $K$ transition matrices from $\mathcal{M}$ to $\mathcal{M}^K$ that compose a discrete memoryless MAC. Mathematically speaking, the probability of observing energy level $j$ when tag $k$ at status $m_k$ is

$$P(\bar{z}_j \mid \bar{c}_{m_k}) = \frac{\sum_{m_{K \setminus k}} P(\bar{z}_j \mid \bar{c}_{m_K})}{\sum_{m_K} P(\bar{z}_j \mid \bar{c}_{m_K})}. \tag{13}$$

In summary, for every possible tag input combination, the expected power of the received signal per block can be evaluated by (6), the energy detection threshold to nearby states can be computed by (24), the decision region can be retrieved by (25), the equivalent point-to-point channel can be obtained by (11) and (12), and the discrete memoryless MAC can be extracted by (13).

### C. Backscatter sum-capacity

Before investigating the sum-capacity of the tags, we introduce some prerequisites in information theory. Define the input probability distribution of tag $k$ at status $m_k$ as $P_k(\bar{c}_{m_k})$, and assume the input distribution of all tags are mutually independent, such that $P_K(\bar{c}_{m_K}) = \prod_{k \in \mathcal{K}} P_k(\bar{c}_{m_k})$. Following [12], the information function associated with specific tag input combination $\bar{c}_{m_K}$ is defined as

$$I(\bar{c}_{m_K}; z) \triangleq \sum_j P(\bar{z}_j \mid \bar{c}_{m_K}) \log \frac{P(\bar{z}_j \mid \bar{c}_{m_K})}{P(\bar{z}_j)}, \tag{14}$$

the marginal information function on $\mathcal{S} \subset \mathcal{K}$ can be written as

$$I_{\mathcal{S}}(\bar{c}_{m_{\mathcal{S}}}; z) = \sum_{m_{K \setminus \mathcal{S}}} P_{K \setminus \mathcal{S}}(\bar{c}_{m_{K \setminus \mathcal{S}}}) I(\bar{c}_{m_K}; z), \tag{15}$$

and the mutual information of the tags and the received signal can be expressed as[8]

$$I(c_K; z) = \mathbb{E}_{c_K}[I(\bar{c}_{m_K}; z)] = \mathbb{E}_{c_{\mathcal{S}}}[I_{\mathcal{S}}(\bar{c}_{m_{\mathcal{S}}}; z)]. \tag{16}$$

Evidently, for a given discrete memoryless MAC with transition probability $P(z \mid c_K)$, the information function $I(\bar{c}_{m_K}; z)$ and mutual information $I(c_K; z)$ only depend on the tag input distribution $P_k(\bar{c}_{m_k})$, $\forall m_k \in \mathcal{M}$, $\forall k \in \mathcal{K}$. Therefore, we can obtain the backscatter sum-capacity by maximizing the mutual information over the tag input distributions as

$$R_c = \max_{P(c_K)} I(c_K; z) \text{ [bpcu]}. \tag{17}$$

### D. Primary ergodic capacity

Once the tag symbol set $\bar{c}_{m_K}$ is successfully decoded, the user can eliminate the backscatter uncertainty and model it within the equivalent primary channel by (5). From the perspective of primary transmission, the tags adjust the propagation environment in a potentially beneficial manner, and create artificial channel variation within each fading block. As such, the ergodic primary capacity can be expressed as

$$R_s = \mathbb{E}_{c_K}\left[\log_2\left(1 + \frac{|\boldsymbol{h}_E^H(c_K)\boldsymbol{w}|^2}{\sigma_w^2}\right)\right]$$
$$= \sum_{m_K}\prod_{k \in \mathcal{K}} P_k(\bar{c}_{m_K}) \log_2\left(1 + \frac{|\boldsymbol{h}_E^H(\bar{c}_{m_K})\boldsymbol{w}|^2}{\sigma_w^2}\right) \text{ [bps/Hz]}. \tag{18}$$

which is also a function of the tag input distribution $P(c_K)$.

### III. TAG INPUT AND PRECODER DESIGN

#### A. Primary ergodic-secondary sum rate region

To achieve a flexible tradeoff between the primary and backscatter links, we aim to optimize the precoder and tag input distribution to maximize the weighted sum of the ergodic primary rate and the total backscatter rate, under the average transmit power and probability constraints

$$\max_{P(c_K),\boldsymbol{w}} \quad \rho R_s + (1-\rho)R_c \tag{19a}$$
$$\text{s.t.} \quad \|\boldsymbol{w}\|^2 \leq P, \tag{19b}$$
$$\sum_{m_k} P_k(\bar{c}_{m_k}) = 1, \quad \forall k \in \mathcal{K}, \tag{19c}$$
$$P_k(\bar{c}_{m_k}) \geq 0, \quad \forall m_k \in \mathcal{M}, \forall k \in \mathcal{K} \tag{19d}$$

where $\rho \in [0,1]$ denotes the priority of the primary link. As problem (19) is not jointly convex over $\boldsymbol{w}$ and $P(c_K)$, we propose an alternating optimization (AO)-based algorithm that iteratively retrieve the global optimal precoder and capacity-achieving input distribution in closed forms.

#### B. Precoder

TODO

---

[7]For simplicity, we assume there exists at least one feasible precoder that produces distinct received energy levels for all tag input combinations. [TODO] Is this necessary? Maybe we can keep those same energy levels and avoid them by input distribution design.

[8]Please be aware that $c_K$, $c_{\mathcal{S}}$, $z$ are random variables, while $\bar{c}_{m_K}$ (and $\bar{c}_i$), $\bar{c}_{m_{\mathcal{S}}}$, $\bar{z}_j$ represent the corresponding instances.

## IV. THE SINGLE-TAG CASE

As shown in Fig. NULL, we propose a single-user (UE) single-tag (TG) symbiotic radio network where the RF signal generated by the single-antenna Access Point (AP) is shared by two coexisting systems. In the primary AP-UE downlink system, the AP transmits to the single-antenna user. In the secondary AP-TG-UE backscatter system, the AP acts as the carrier emitter, the user serves as the backscatter reader, and the single-antenna tag modulates its information over the reradiated RF signal by varying the reflection coefficient. Denote the AP-UE direct channel as $h_D$, the AP-TG forward channel as $h_F$, and the TG-UE backward channel as $h_B$. We consider the quasi-static block fading model and assume the CSI of the direct channel and the cascaded forward-backward channel $h_C \triangleq h_B h_F$ are known at the AP.[9] It is assumed that the primary symbol $s$ follows standard CSCG distribution $\mathcal{CN}(0,1)$ and the secondary symbol $c$ employs $M$-PSK modulation by (2). Due to the practical constraints on switching speed and synchronization gap, the passive tag typically transmits at a much lower data rate than the AP. Hence, we assume the secondary symbol period is $N \gg 1 \in \mathbb{Z}_{++}$ times the primary symbol period and focus on the interval of one particular $c$. At (primary) symbol block $n \in \mathcal{N} \triangleq \{1, \ldots, N\}$, the user simultaneously captures the signal from both primary and secondary links as[10]

$$y[n] = \sqrt{P} h_D s[n] + \sqrt{\alpha P} h_C c s[n] + w[n], \quad (20)$$

where $P$ is the average transmit power at the AP and $w \sim \mathcal{CN}(0, \sigma^2)$ is the additive white Gaussian noise. We also define $\boldsymbol{y} \triangleq \left[y[1], \ldots, y[N]\right]^T$.

**Remark 4.** *The symbiotic radio network can be regarded as a special case of Multiple Access Channel (MAC) because the AP and the tag simultaneously transmit to the user. It is known that Superposition Coding-Successive Interference Cancellation (SC-SIC) with different decoding orders can achieve different vertices of the MAC capacity region [15]. Therefore, most relevant papers proposed the user to first decode the primary message (by treating the tag interference as noise), cancel out its contribution from the received signal, then decode the secondary message. Since the direct channel is typically much stronger than the cascaded channel [16], the primary decoding is expected to enjoy a high Signal-to-Interference-and-Noise Ratio (SINR) and the secondary decoding is ideally interference-free.*

**Remark 5.** *The main difference between symbiotic radio and conventional MAC is that the primary message also reaches the user from the backscatter link. This characteristic inspires one to first decode the tag message, then model its contribution within the equivalent channel during primary decoding (i.e., unify backscatter decoding and channel training), instead of performing SIC. In such case, the reflection pattern not only embeds the tag message but also adjusts the legacy channel in a controllable manner. Therefore, for a fixed fading block, the primary transmission is able to achieve the ergodic capacity with artificial channel variation created by the backscatter modulation. [Channel over channel, randomness over randomness]*

### A. Backscatter Transmission

To investigate how backscatter modulation potentially benefits the primary transmission, we first decode the tag symbol $c$ in presence of the interference from the primary message $s$. In such case, the detection indeed coincides with that of Ambient Backscatter Communications (AmBC) where the signaling from the ambient source is unknown, and the received signal per symbol block follows the CSCG distribution of $y_m[n] \sim \mathcal{CN}(0, \sigma_m^2)$, where

$$\sigma_m^2 \triangleq |h_D + \sqrt{\alpha} h_C c_m|^2 P + \sigma^2 \quad (21)$$

denotes the typical received signal energy over $N$ symbol blocks when the tag is at state $m$, which can be estimated at the user. For the ease of exposition, we sort $\{\sigma_m^2\}$ in a ascending order by bijective mapping $f: m \mapsto i$[11] and let $\sigma_i^2 \leq \sigma_j^2$ for $i < j$, $i, j \in \mathcal{M}$. Denote $\mathcal{H}_i$ as the hypothesis that the tag transmits $c_i$. Following [11], the optimal Maximum-Likelihood (ML) detector boils down to the energy detector, and the likelihood ratio between hypotheses $\mathcal{H}_i$ and $\mathcal{H}_j$ is

$$\Lambda_{i,j}(\boldsymbol{y}) = \frac{f(\boldsymbol{y} \mid \mathcal{H}_i)}{f(\boldsymbol{y} \mid \mathcal{H}_j)} = \left(\frac{\sigma_j^2}{\sigma_i^2}\right)^N \exp\left(\frac{(\sigma_i^2 - \sigma_j^2)z}{\sigma_i^2 \sigma_j^2}\right), \quad (22)$$

where $f(\boldsymbol{y} \mid \mathcal{H}_i)$, $f(\boldsymbol{y} \mid \mathcal{H}_j)$ denote respectively the conditional probability density function of receiving $\boldsymbol{y}$ under hypothesis $\mathcal{H}_i$ and $\mathcal{H}_j$, and $z \triangleq \|y\|^2$ is the received signal energy over $N$ symbol blocks. The corresponding decision rule is

$$\Lambda_{i,j}(\boldsymbol{y}) \underset{H_j}{\overset{H_i}{\lessgtr}} 1 \iff z \underset{H_j}{\overset{H_i}{\lessgtr}} T_{i,j}, \quad (23)$$

where the optimal detection threshold is

$$T_{i,j} \triangleq N \frac{\sigma_i^2 \sigma_j^2}{\sigma_i^2 - \sigma_j^2} \log \frac{\sigma_i^2}{\sigma_j^2}, \quad (24)$$

and the decision region of hypothesis $\mathcal{H}_i$ can be expressed as

$$\mathcal{R}_i \triangleq [T_{i-1,i}, T_{i,i+1}), \quad (25)$$

with $T_{0,1} \triangleq 0$ and $T_{M,M+1} \triangleq \infty$. On top of this, we define the forward transition probability matrix $\boldsymbol{P} \in \mathbb{R}_+^{M \times M}$ as

$$\boldsymbol{P} \triangleq \begin{bmatrix} p_{1,1} & \cdots & p_{1,M} \\ \vdots & \ddots & \vdots \\ p_{M,1} & \cdots & p_{M,M} \end{bmatrix}, \quad (26)$$

where $p_{i,j}$ denotes the transition probability from channel input state $i$ to output state $j$. It can be derived as

$$p_{i,j} = p(z \in \mathcal{R}_j \mid \mathcal{H}_i) = \int_{\mathcal{R}_j} f(z \mid \mathcal{H}_i) \mathrm{d}z, \quad (27)$$

---

[9]Due to the lack of RF chains at the passive tag, accurate and efficient CSI acquisition at the AP can be challenging. One possible approach is that the AP sends known pilots, the tag responds in a pre-defined manner, and the user performs least-square estimation then feeds back to the AP [6]–[8].

[10]We assume the time difference of arrival from the AP-UE path and the AP-TG-UE path are negligible compared to the symbol period [10], [13], [14].

[11]Note that the mapping is not unique and the detection fails when two different constellation points yield the same energy level.

where $f(z \mid \mathcal{H}_i)$ is the conditional probability density function of receiving $z$ under hypothesis $\mathcal{H}_i$. Since $z$ follows chi-squared distribution with $2N$ degrees of freedom, it holds that

$$f(z \mid \mathcal{H}_i) = \frac{z^{N-1}e^{-z/\sigma_i^2}}{\sigma_i^{2N}\Gamma(N)}, \tag{28}$$

where $\Gamma(\cdot)$ is the gamma function. To summarize, with the CSI of the direct and cascaded links, the typical energy of the received signal can be estimated by (21), the energy detection threshold can be computed by (24), the decision region can be retrieved by (25), and the forward transition matrix $\boldsymbol{P}$ can be calculated by substituting (28) into (27).

We then investigate the achievable rate of the backscatter link. Denote the tag input probability mass function as $\boldsymbol{r} = [r_1, \ldots, r_M]^T \in \mathbb{R}_+^{M \times 1}$ where $r_m$ is the probability to transmit symbol $c_m$ [strictly positive?]. For a given input distribution $\boldsymbol{r}$ and forward transition matrix $\boldsymbol{P}$, the achievable backscatter rate can be written as

$$R_c = \max_{\boldsymbol{Q} \geq 0} \sum_{i \in \mathcal{M}} \sum_{j \in \mathcal{M}} r_i p_{i,j} \log_2 \frac{q_{j,i}}{r_i} \text{ [bpcu]}, \tag{29}$$

where $\boldsymbol{Q} \in \mathbb{R}_+^{M \times M}$ is the backward transition probability matrix

$$\boldsymbol{Q} \triangleq \begin{bmatrix} q_{1,1} & \cdots & q_{1,M} \\ \vdots & \ddots & \vdots \\ q_{M,1} & \cdots & q_{M,M} \end{bmatrix}, \tag{30}$$

and $q_{j,i}$ denotes the transition probability from channel output state $j$ to input state $i$.

### B. Legacy Transmission

Once the backscattered symbol is successfully recovered, it is combined with the cascaded channel to eliminate the uncertainty of the AP-TG-UE path and assist the legacy transmission. Therefore, the received signal at symbol block $n$ is essentially

$$y[n] = \sqrt{P}(h_{\mathrm{D}} + \sqrt{\alpha}h_{\mathrm{C}}c)s[n] + w[n] \triangleq \sqrt{P}h_{\mathrm{E}}(c)s + w[n], \tag{31}$$

which is reminiscent of an IRS-aided point-to-point transmission with an equivalent channel of

$$h_{\mathrm{E}}(c) \triangleq h_{\mathrm{D}} + \sqrt{\alpha}h_{\mathrm{C}}c. \tag{32}$$

For primary transmission, backscatter modulation creates an artificial fast fading within each fading block, and AP can obtain the equivalent CSI distribution for any given tag input probability mass function $\boldsymbol{r}$. Therefore, the ergodic capacity of primary transmission within each symbol block is [17]

$$R_s = \mathbb{E}_c\big[\log_2(1 + \gamma|h_{\mathrm{E}}(c)|^2)\big]$$
$$= \sum_{i \in \mathcal{M}} r_i \log_2\big(1 + \gamma|h_{\mathrm{D}} + \sqrt{\alpha}h_{\mathrm{C}}c_i|^2\big) \text{ [bps/Hz]}, \tag{33}$$

where $\gamma \triangleq P/\sigma^2$ is the average transmit Signal-to-Noise Ratio (SNR). It can be concluded that the achievable rate of both primary and secondary links depend on the tag input distribution.

### C. Achievable rate region

To achieve a flexible tradeoff between the backscatter and legacy links, we aims to optimize the tag input probability mass function, under $M$-PSK modulation, to maximize the weighted sum of the primary and secondary rates subject to the sum-probability constraint

$$\max_{\boldsymbol{r} \geq 0} \quad \rho R_s + (1-\rho)R_c \tag{34a}$$

$$\text{s.t.} \quad \sum_{i \in \mathcal{M}} r_i = 1, \tag{34b}$$

where $\rho \in [0,1]$ is the weight factor. By substituting (29) and (33) into (34a), the problem expands to

$$\max_{\boldsymbol{r} \geq 0, \boldsymbol{Q} \geq 0} \quad \rho \sum_{i \in \mathcal{M}} r_i \log_2\big(1 + \gamma|h_{\mathrm{D}} + \sqrt{\alpha}h_{\mathrm{C}}c_i|^2\big)$$
$$+ (1-\rho) \sum_{i \in \mathcal{M}} \sum_{j \in \mathcal{M}} r_i p_{i,j} \log_2 \frac{q_{j,i}}{r_i} \tag{35a}$$

$$\text{s.t.} \quad \sum_{i \in \mathcal{M}} r_i = 1. \tag{35b}$$

Similar to the Blahut-Arimoto algorithm [18], [19], we optimize $\boldsymbol{r}$ and $\boldsymbol{Q}$ alternately to obtain the local optimal tag input distribution and the corresponding weighted sum-rate.

**Theorem 1.** *For any valid tag input probability mass function $\boldsymbol{r}$ [$\boldsymbol{r} > 0$?], the optimal backward transition probability from channel output state $j$ to input state $i$ follows Bayes' Theorem as*

$$q_{j,i}^\star = \frac{r_i p_{i,j}}{\sum_{i'} r_{i'} p_{i',j}}. \tag{36}$$

*Proof.* Please refer to Appendix A. $\square$

**Theorem 2.** *For any valid backward transition probability $\boldsymbol{Q}$ [$\boldsymbol{Q} \geq 0$?], the optimal tag input probability mass function is given by*

$$r_i = \frac{\big(1 + \gamma|h_{\mathrm{D}} + \sqrt{\alpha}h_{\mathrm{C}}c_i|^2\big)^{\rho/(1-\rho)} \prod_{j \in \mathcal{M}} q_{j,i}^{p_{i,j}}}{\sum_{i' \in \mathcal{M}} \big(1 + \gamma|h_{\mathrm{D}} + \sqrt{\alpha}h_{\mathrm{C}}c_{i'}|^2\big)^{\rho/(1-\rho)} \prod_{j \in \mathcal{M}} q_{j,i'}^{p_{i',j}}}. \tag{37}$$

*Proof.* Please refer to Appendix B. $\square$

**Proposition 1.** *For any feasible initial point [constellation subset], the Algorithm is guaranteed to converge to the global optimal of problem (34) and achieve the maximum weighted-sum rate.*

*Proof.* The proof is similar to that in [20, Chapter 9.3] and omitted here. $\square$

## V. OFDM

Due to the constraint of energy detection, with single-antenna tags and reader, at most one AmBC tag can be decoded at a time and accurate detection requires repetition coding over multiple time/frequency blocks to mitigate the impact of primary symbols. Here we consider frequency-independent tag reflection and schedule one tag per OFDM symbol.

At OFDM symbol $r$, tag $l$ modulates its own information over all $N$ subcarriers while the remaining tags may operate in the cooperative (quantized IRS) mode. Channel frequency response at subband $n$ and block $r$ Received signal at OFDM symbol $r$ and subband $n$ is

$$y_n[r] = \sqrt{P}h_{\mathrm{E}}[r]s_n[r] + \sqrt{\alpha P}h_{\mathrm{C},l}c_l s_n[r] + w_n[r], \quad (38)$$

where $h_{\mathrm{E}}[r] \triangleq \sum_{l' \neq l} h_{\mathrm{C},l'}c_{l'}^{\star}$ and $c_l$ is the symbol of tag $l$. Apparently $y_n[r] \sim \mathcal{CN}(0, \sigma_n^2[r])$ with $\sigma_n^2[r] \triangleq |h_{\mathrm{E}}[r] + \sqrt{\alpha}h_{\mathrm{C},l}c_l|^2 P + \sigma^2$. Define $\boldsymbol{y}[r] \triangleq [y_1[r], \ldots, y_N[r]]^T$ and we can do energy detection over $N$ subcarriers.

## VI. Multi-Tag Case

In the $K$-tag scenario, the received signal at symbol block $n$ is

$$y[n] = \sqrt{P}h_{\mathrm{D}}s[n] + \sum_k \sqrt{\alpha_k}h_{\mathrm{C},k}c_k\sqrt{P}s[n] + w[n]. \quad (39)$$

On the one hand, we can compute the *sum-rate* of the tags and characterize the (ergodic) primary-secondary capacity region by adjusting weight $\rho$. The weighted sum-rate can be expressed as

$$J_1 = \rho\mathbb{E}_{\boldsymbol{c}}\left[\log_2\left(1 + \gamma|h_{\mathrm{D}} + \sum_k \sqrt{\alpha_k}h_{\mathrm{C},k}c_k|\right)\right] + (1-\rho)R_c \tag{40}$$

$$= \rho \sum_{i_1,\ldots,i_K \in \mathcal{M}} \prod_{k \in \mathcal{K}} r_{k,i_k} \log_2\left(1 + \gamma|h_{\mathrm{D}} + \sum_{k' \in \mathcal{K}} \sqrt{\alpha_{k'}}h_{\mathrm{C},k'}c_{k',i_{k'}}|^2\right) \tag{41}$$

$$+ (1-\rho) \sum_{i \in \mathcal{M}} \sum_{j \in \mathcal{M}^K} \sum_{k \in \mathcal{K}} r_{k,i}p_{i,j}\log\frac{q_{j,i}}{r_{k,i}}. \tag{42}$$

In this case, although we can independently maximize the primary/secondary rate in closed form (resp. quantized IRS and multi-user Blahut-Arimoto), the joint form can be tricky due to the $K$-product term. We may consider a 2-loop iterative algorithm, where the inner loop optimizes input distribution over letters while the outer loop over users. I am still working on the convergence and optimality proofs and they are very deep into information theory.

On the other hand, we can compute the rate region of the user and $K$ tags. However, the capacity region of discrete MAC remains unknown. We can obtain its outer bound by formulating a non-convex problem with a rank-1 constraint, then solve the relaxed problem. The difficulty is that the optimization is performed over $K$-dimensional array $\mathbb{R}^{\overbrace{M \times \ldots \times M}^{K}}$.

## Appendix

### A. Proof of Theorem 1

Denote the objective function (35a) as $R(\boldsymbol{r}, \boldsymbol{Q})$. Let $w_j \triangleq \sum_{i'} r_{i'}p_{i',j}$ and rearrange (36) as

$$w_j q_{j,i}^{\star} = r_i p_{i,j}. \tag{43}$$

Therefore,

$$\begin{aligned}
R(\boldsymbol{r}, \boldsymbol{Q}^{\star}) - R(\boldsymbol{r}, \boldsymbol{Q}) &= (1-\rho) \sum_{i \in \mathcal{M}} \sum_{j \in \mathcal{M}} r_i p_{i,j} \log_2 \frac{q_{j,i}^{\star}}{q_{j,i}} \\
&= (1-\rho) \sum_{i \in \mathcal{M}} \sum_{j \in \mathcal{M}} w_j q_{j,i}^{\star} \log_2 \frac{q_{j,i}^{\star}}{q_{j,i}} \\
&= (1-\rho) \sum_{j \in \mathcal{M}} w_j \sum_{i \in \mathcal{M}} q_{j,i}^{\star} \log_2 \frac{q_{j,i}^{\star}}{q_{j,i}} \\
&= (1-\rho) \sum_{j \in \mathcal{M}} w_j D(q_{j,i}^{\star} \parallel q_{j,i}) \\
&\geq 0, \tag{44}
\end{aligned}$$

with equality iff $\boldsymbol{Q} = \boldsymbol{Q}^{\star}$.

### B. Proof of Theorem 2

We employ the method of Lagrange multipliers, temporally ignore the constraint $\boldsymbol{r} \geq 0$, and assume all logarithms are of base $e$. Define the Lagrangian function as

$$\begin{aligned}
J &= \rho \sum_{i \in \mathcal{M}} r_i \log\left(1 + \gamma|h_{\mathrm{D}} + \sqrt{\alpha}h_{\mathrm{C}}c_i|^2\right) \\
&+ (1-\rho) \sum_{i \in \mathcal{M}} \sum_{j \in \mathcal{M}} r_i p_{i,j}\log\frac{q_{j,i}}{r_i} + \lambda\left(1 - \sum_{i \in \mathcal{M}} r_i\right), \tag{45}
\end{aligned}$$

where $\lambda$ is the Lagrange multiplier associated with the sum-probability constraint. Differentiating $J$ with respect to $r_i$ gives

$$\frac{\partial J}{\partial r_i} = \rho \log\left(1 + \gamma|h_{\mathrm{D}} + \sqrt{\alpha}h_{\mathrm{C}}c_i|^2\right) \tag{46}$$

$$+ (1-\rho)\left(\sum_{j \in \mathcal{M}} p_{i,j}\log q_{j,i} - \log r_i - 1\right), \tag{47}$$

and setting $\partial J/\partial r_i = 0$ suggests

$$r_i = e^{-(\frac{\lambda}{1-\rho}+1)}\left(1 + \gamma|h_{\mathrm{D}} + \sqrt{\alpha}h_{\mathrm{C}}c_i|^2\right)^{\rho/(1-\rho)} \prod_{j \in \mathcal{M}} q_{j,i}^{p_{i,j}}. \tag{48}$$

By considering $\sum_{i \in \mathcal{M}} r_i = 1$, we can eliminate $\lambda$ and obtain the optimal tag input distribution as (37).

## References

[1] J. Kim and B. Clerckx, "Wireless Information and Power Transfer for IoT: Pulse Position Modulation, Integrated Receiver, and Experimental Validation," *arXiv:2104.08404*, pp. 1–15, apr 2021. [Online]. Available: http://arxiv.org/abs/2104.08404

[2] R. Hansen, "Relationships Between Antennas as Scatterers and as Radiators," *Proceedings of the IEEE*, vol. 77, no. 5, pp. 659–662, may 1989. [Online]. Available: http://ieeexplore.ieee.org/document/32056/

[3] C. Boyer and S. Roy, "Backscatter Communication and RFID: Coding, Energy, and MIMO Analysis," *IEEE Transactions on Communications*, vol. 62, no. 3, pp. 770–785, mar 2014. [Online]. Available: http://ieeexplore.ieee.org/document/6685977/

[4] D. M. Dobkin, *The RF in RFID: UHF RFID in Practice*. Newnes, 2012.

[5] S. J. Thomas, E. Wheeler, J. Teizer, and M. S. Reynolds, "Quadrature Amplitude Modulated Backscatter in Passive and Semipassive UHF RFID Systems," *IEEE Transactions on Microwave Theory and Techniques*, vol. 60, no. 4, pp. 1175–1182, apr 2012. [Online]. Available: http://ieeexplore.ieee.org/document/6153042/

[6] D. Bharadia, K. R. Joshi, M. Kotaru, and S. Katti, "BackFi: High Throughput WiFi Backscatter," in *Proceedings of the 2015 ACM Conference on Special Interest Group on Data Communication*, vol. 45, no. 4. New York, NY, USA: ACM, aug 2015, pp. 283–296. [Online]. Available: https://dl.acm.org/doi/10.1145/2785956.2787490

[7] G. Yang, C. K. Ho, and Y. L. Guan, "Multi-Antenna Wireless Energy Transfer for Backscatter Communication Systems," *IEEE Journal on Selected Areas in Communications*, vol. 33, no. 12, pp. 2974–2987, dec 2015. [Online]. Available: http://ieeexplore.ieee.org/document/7274644/

[8] H. Guo, Q. Zhang, S. Xiao, and Y.-C. Liang, "Exploiting Multiple Antennas for Cognitive Ambient Backscatter Communication," *IEEE Internet of Things Journal*, vol. 6, no. 1, pp. 765–775, feb 2019. [Online]. Available: https://ieeexplore.ieee.org/document/8411483/

[9] Q. Wu and R. Zhang, "Intelligent Reflecting Surface Enhanced Wireless Network via Joint Active and Passive Beamforming," *IEEE Transactions on Wireless Communications*, vol. 18, no. 11, pp. 5394–5409, nov 2019. [Online]. Available: https://ieeexplore.ieee.org/document/8811733/

[10] H. Guo, Y.-C. Liang, R. Long, and Q. Zhang, "Cooperative Ambient Backscatter System: A Symbiotic Radio Paradigm for Passive IoT," *IEEE Wireless Communications Letters*, vol. 8, no. 4, pp. 1191–1194, aug 2019. [Online]. Available: https://ieeexplore.ieee.org/document/8692391/

[11] J. Qian, A. N. Parks, J. R. Smith, F. Gao, and S. Jin, "IoT Communications With M-PSK Modulated Ambient Backscatter: Algorithm, Analysis, and Implementation," *IEEE Internet of Things Journal*, vol. 6, no. 1, pp. 844–855, feb 2019. [Online]. Available: https://ieeexplore.ieee.org/document/8423609/

[12] M. Rezaeian and A. Grant, "Computation of Total Capacity for Discrete Memoryless Multiple-Access Channels," *IEEE Transactions on Information Theory*, vol. 50, no. 11, pp. 2779–2784, nov 2004. [Online]. Available: http://ieeexplore.ieee.org/document/1347364/

[13] Y.-C. Liang, Q. Zhang, E. G. Larsson, and G. Y. Li, "Symbiotic Radio: Cognitive Backscattering Communications for Future Wireless Networks," *IEEE Transactions on Cognitive Communications and Networking*, vol. 6, no. 4, pp. 1242–1255, dec 2020. [Online]. Available: https://ieeexplore.ieee.org/document/9193946/

[14] R. Long, Y.-C. Liang, H. Guo, G. Yang, and R. Zhang, "Symbiotic Radio: A New Communication Paradigm for Passive Internet of Things," *IEEE Internet of Things Journal*, vol. 7, no. 2, pp. 1350–1363, feb 2020. [Online]. Available: https://ieeexplore.ieee.org/document/8907447/

[15] A. Goldsmith, *Wireless Communications*. Cambridge University Press, 2005. [Online]. Available: https://books.google.co.uk/books?id=ZtFVAgAAQBAJ

[16] O. Ozdogan, E. Bjornson, and E. G. Larsson, "Intelligent Reflecting Surfaces: Physics, Propagation, and Pathloss Modeling," *IEEE Wireless Communications Letters*, vol. 9, no. 5, pp. 581–585, may 2020. [Online]. Available: https://ieeexplore.ieee.org/document/8936989/

[17] D. Tse and P. Viswanath, *Fundamentals of Wireless Communication*. Cambridge University Press, may 2005. [Online]. Available: https://www.cambridge.org/core/product/identifier/9780511807213/type/book

[18] S. Arimoto, "An Algorithm for Computing the Capacity of Arbitrary Discrete Memoryless Channels," *IEEE Transactions on Information Theory*, vol. 18, no. 1, pp. 14–20, jan 1972. [Online]. Available: http://ieeexplore.ieee.org/document/1054753/

[19] R. Blahut, "Computation of Channel Capacity and Rate-Distortion Functions," *IEEE Transactions on Information Theory*, vol. 18, no. 4, pp. 460–473, jul 1972. [Online]. Available: http://ieeexplore.ieee.org/document/1054855/

[20] R. W. Yeung, *Information Theory and Network Coding*, ser. Information Technology: Transmission, Processing and Storage. Springer US, 2008. [Online]. Available: https://books.google.co.uk/books?id=Mj4iC5-FQWgC